New Approach to Low-Cost Dye-Sensitized Solar Cells With Back Contact Electrodes

Nobuhiro Fuke,*,[†] Atsushi Fukui,[†] Ryohichi Komiya,[†] Ashraful Islam,[†] Yasuo Chiba,[†] Masatoshi Yanagida,[‡] Ryohsuke Yamanaka,[†] and Liyuan Han*,[†]

Advanced Energy Laboratories, Sharp Corporation, Hajikami 282-1, Katsuragi-shi, Nara, 639-2198, Japan, and National Institute of Advanced Industrial Science and Technology (AIST), Tsukuba Central 5, 1-1-1 Higashi, Tsukuba, Ibaraki, 305-8565, Japan

Much attention has been paid to the development of dye-sensitized solar cells (DSCs) owing to a possibility of low production cost. One of the main factors that has hampered the practical application of DSCs is the use of a transparent conducting oxide (TCO) substrate of very high cost. Here we introduce a newly structured DSC back contact dye-sensitized solar cell (BCDSC) in which the TCO is omitted and a porous Ti electrode for electron collection, called a back contact electrode (BCE), is placed on the side opposite to the side of light irradiation. We succeeded in fabricating on the TiO2 film a BCE with large enough pore size for both efficient dye adsorption onto the film and smooth I^-/I_3^- redox couple transportation through the film. Electrochemical impedance spectroscopy study showed that increase in the BCE thickness causes increase in the I^-/I_3^- redox couple transport resistance at the same time as reduction of BCE resistance. Under standard air mass (AM) 1.5 irradiation (100 mW cm^{-2}), a BCDSC with N719 dye yielded an overall conversion efficiency of 8.4%. An intensity modulated photovoltage spectroscopy (IMVS) study indicated that the lifetime of electrons in the TiO$_2$ film of the BCDSC is long enough for them to reach the BCE. The BCDSC therefore has the potential for high photovoltaic performance even though the TiO$_2$ film contains many interfaces between TiO$_2$ particles such as the grain boundary in the polycrystalline silicon. The high-efficiency BCDSC achieved in the present study brings a low-cost DSC one step closer to practical use.

Introduction

Dye-sensitized nanocrystalline solar cells (DSCs) have the potential to deliver short energy-payback time at low cost and may offer an alternative to conventional semiconductor-based photovoltaic devices. As shown in Figure 1a, DSCs consist of a mesoporous nanocrystalline titanium dioxide (TiO$_2$) film electrode deposited on a transparent conducting oxide (TCO), a monolayer of dye adsorbed onto the TiO$_2$, a platinum (Pt) counter electrode, and an electrolyte solution with a dissolved iodide/triiodide (I^-/I_3^-) redox couple in between the electrodes. When the DSC is irradiated by sunlight, the dye is excited and injects electrons into the conduction band of the TiO$_2$ which pass through the nanoparticles of the TCO into the external circuit. The oxidized dye is then reduced back and hole transported to a Pt counter electrode by the (I^-/I_3^-) redox couple. During the past decade, there have been wide-ranging investigations to achieve high energy conversion efficiency.[1–4] It is well-established that practical use requires improvement in three

areas: conversion efficiency, long-term stability, and fabrication cost relative to silicon solar cells. DSCs have achieved energy conversion efficiency of over 11% at solar irradiation of air mass (AM) 1.5[5,6] and long-term stability under stress conditions.[7–9] There have however been no studies aimed at fabrication cost reduction. The main cost factor in DSCs is the TCO substrate material, which accounts for 24% of the total fabrication cost.[10] A new DSC structure without TCO is therefore required to cut fabrication costs.

In the case of single-crystalline silicon solar cells, in order to reduce the incident light loss at the front electrode caused by light reflection and absorption, a point contact silicon solar cell[11] and a back contact solar cell[12] (BCS) have been introduced as new types of silicon solar cells in which electrodes are placed on the side opposite to the side of light

* Corresponding authors. E-mail: fuke.nobuhiro@sharp.co.jp (N.F.), han.liyuan@sharp.co.jp (L.H.). Tel.: +81-745-63-3539. Fax: +81-745-63-3306.
† Sharp Corporation.
‡ National Institute of Advanced Industrial Science and Technology (AIST).

(1) O'Regan, B.; Grätzel, M. *Nature* 1991, *353*, 737.
(2) Nazeeruddin, M. d. K.; Kay, A.; Rodicio, I.; Humphry-Baker, R.; Müller, E.; Liska, P.; Vlachopoulos, N.; Grätzel, M. *J. Am. Chem. Soc.* 1993, *115*, 6382.
(3) Grätzel, M. *J. Photochem. Photobiol., A* 2004, *164*, 3.
(4) Grätzel, M. *J. Photochem. Photobiol., C* 2003, *4*, 145.
(5) Nazeeruddin, M. K.; Angelis, F. D.; Fantacci, S.; Selloni, A.; Viscardi, G.; Liska, P.; Ito, S.; Bessho, T.; Grätzel, M. *J. Am. Chem. Soc.* 2005, *127*, 16835.
(6) Chiba, Y.; Islam, A.; Watanabe, Y.; Komiya, R.; Koide, N.; Han, L. *Jpn. J. Appl. Phys.* 2006, *45* (25), L638.
(7) Hara, K.; Kurashige, M.; Ito, S.; Shinpo, A.; Suga, S.; Sayama, K.; Arakawa, H. *Chem. Commun.* 2003, *2*, 252.
(8) Wang, P.; Zakeeruddin, S. M.; Moser, J. E.; Nazeeruddin, M. K.; Sekiguchi, T.; Grätzel, M. *Nat. Mater.* 2003, *2*, 402.
(9) Mazille, F.; Fei, Z.; Kuang, D.; Zhao, D.; Zakeeruddin, S. M.; Grätzel, M.; Dyson, P. J. *Inorg. Chem.* 2006, *45*, 1585.
(10) Kroon, J. M.; Bakker, N. J.; Smit, H. J. P.; Liska, P.; Thampi, K. R.; Wang, P.; Zakeeruddin, S. M.; Grätzel, M.; Hinsch, A.; Hore, S.; Würfel, U.; Sastrawan, R.; Durrant, J. R.; Palomares, E.; Pettersson, H.; Gruszecki, T.; Walter, J.; Skupien, K.; Tulloch, G. E. *Prog. Photovoltaics Res. Appl.* 2007, *15*, 1.
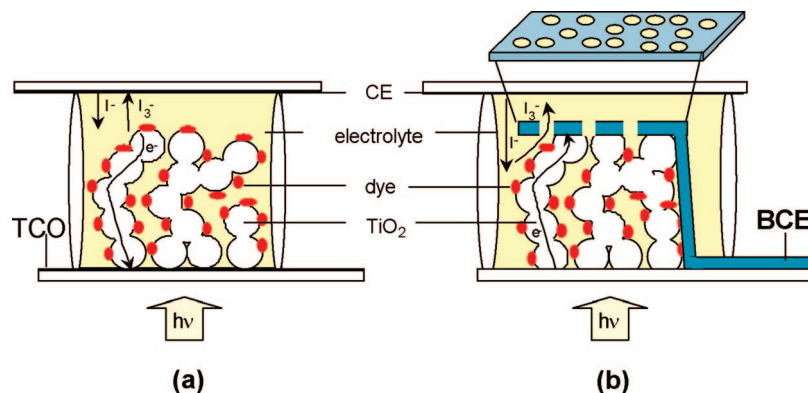
Figure 1. (a) Cross-sectional sketch of a dye-sensitized solar cell and (b) back contact dye-sensitized solar cell.

irradiation. The back contact (BC) concept cannot, however, be applied to polycrystalline silicon solar cells because of the very short carrier lifetime.

In the present paper, we introduce a newly structured DSC, called a BCDSC, in which the back contact structure is applied to allow the TCO to be omitted.[10,13] We report in detail on methods of BCDSC fabrication and use electrochemical impedance spectroscopy (EIS) measurement to investigate the internal resistance of BCDSC as a way of elucidating the effect of the back contact electrode on electron collection and I^-/I_3^- redox couple transportation in devices designed to improve conversion efficiency. We also investigate electron lifetime in TiO_2 film and show that the back contact structure can be applied to DSCs even though mesoporous nanocrystalline, like polycrystalline silicon film, has many interfaces.

Experimental Details

Fabrication of the Back Contact Dye-Sensitized Solar Cell. BCDSCs were fabricated using a two-electrode sandwich cell configuration. A porous TiO_2 film onto a glass substrate was prepared using a reported method.[14] The thickness of the TiO_2 film was about 15 μm. A back contact electrode of titanium (Ti) is deposited onto the TiO_2 film opposite to the light irradiation side by vacuum deposition (Nihon Sinkuu: EVD-500A). The degree of vacuum was under 1.0×10^{-2} Torr, and substrate rotation speed was 20 rpm. The porous Ti-coated TiO_2 film morphology was investigated using scanning electron microscopy (Philips Co. Ltd. XL30). During measurement several areas were imaged ($\sim$5) to confirm sample uniformity. A dye solution (2×10^{-4} M) of *cis*-dithiocyanato-bis(4,4′-dicarboxy-2,2′-bypyridine)ruthenium(II) $(Bu_4N)_2$ [N719] was prepared in 1:1 acetonitrile and *tert*-butyl alcohol solvents. The electrode was immersed in the dye solution and then kept at 25 °C for 48 h to adsorb the dye onto the TiO_2 surface. A platinum-coated conducting glass was used as the counter electrode. The two electrodes were separated by a Surlyn spacer (50 μm thick) and sealed by heating the polymer frame. The cell gap was kept to 35 μm. The inside of the spacer was filled with electrolyte (0.6 M dimethylpropylimidazolium iodide, 0.05 M I_2,

0.1 M LiI, and 0.5 M *tert*-butylpyridine in acetonitrile) using capillary action.

Electrochemical Impedance Spectroscopy. The electrochemical impedance spectra were measured with an impedance analyzer (Solartron Analytical, 1255B) connected to a potentiostat (Solartron Analytical, 1287) under illumination by a solar simulator (Wacom, WXS-155S-10). EIS spectra were recorded over a frequency range of $10^{-2}-10^6$ Hz at 298 K in a thermostatic chamber. The applied bias voltage and ac amplitude were set at the open-circuit voltage (V_{OC}) of the DSC and 10 mV, respectively. The electrical impedance spectra were characterized using Z-View software (Solartron Analytical).

Intensity Modulated Photovoltage Spectroscopy. Intensity modulated photovoltage spectroscopy (IMVS) of the open circuit was carried out using a combination of sinusoidal low-intensity modulated illumination from a green diode laser (Cobolt Co., Stockholm, Sweden, Samba, 532 nm, 50 mW) and constant-bias light illumination from an Xe lamp (Ushio, Tokyo, Japan, UXL-500D-O), attenuated if necessary with a neutral-density filter. An acoustic optical modulator (Isomet Co., Springfield, VA, 1205C-1) was used to produce sinusoidal modulation of a laser beam. The large perturbation by modulated-light irradiation cannot be described by linear differential equations based on electron lifetime.[15,16] The photocurrent of the cell under modulated-light irradiation was therefore kept below 10% of the whole photocurrent. The amplitude and phase shift of the small sinusoidal photocurrent or photovoltage to the modulated-light irradiation were detected over multidigit modulation frequency using an impedance analyzer (Solartron, Durham, U.K., model 1260 impedance/gain phase analyzer).

Photovoltaic Characterization. The current−voltage characteristics were measured using the previously reported method[17] with a solar simulator (AM 1.5, 100 mW cm^{-2}, WXS-155S-10: Wacom Denso Co. Japan). Monochromatic incident photon-to-current conversion efficiency (IPCE) for the solar cell, plotted as a function of excitation wavelength, was recorded on a CEP-2000 system (Bunkoh-Keiki Co. Ltd.). A black mask (0.2209 cm^2) was attached to the solar cells in order to prevent irradiation with scattering light.

Results and Discussion

The proposed BCDSC structure is shown in Figure 1b. The main difference between DSCs and BCDSCs is the position of the electron collector electrode inside the cell.

(11) Swanson, R. M. *Proceedings of the 17th IEEE Photovoltaics Specialists Conference*, Orlando, May 1984; p 1294.
(12) Campbell, M. P. *Proceedings of the 22nd European Photovoltaic Solar Energy Conference*, Milan, Italy, Sept 2007; p 976.
(13) Fuke, N.; Fukui, A.; Chiba, Y.; Komiya, R.; Yamanaka, R.; Han, L. *Jpn. J. Appl. Phys.* **2007**, *46* (18), L420.
(14) Wang, P.; Zakeeruddin, S. M.; Comte, P.; Charvet, R.; Humphry-Baker, R.; Grätzel, M. *J. Phys. Chem. B* **2003**, *107*, 14336.

(15) Fisher, A. C.; Peter, L. M.; Ponomarev, E. A.; Walker, A. B.; Wijayantha, K. G. U. *J. Phys. Chem. B* **2000**, *104* (5), 949.
(16) Yanagida, M.; Miyamoto, K.; Sayama, K.; Kasuga, K.; Kurashige, M.; Abe, Y.; Sugihara, H. *J. Phys. Chem. C* **2007**, *111*, 201.
(17) Koide, N.; Han, L. *Rev. Sci. Instrum.* **2004**, *75*, 2828.

In the DSC, the TCO works as an electron collector electrode and is located on the light irradiation side of the cell, whereas in the BCDSC a porous Ti metal electrode is located opposite to the light irradiation side, and since it is therefore located on the back of the cell, it is called a back contact electrode (BCE). The usual electrode materials are indium (In), silver (Ag), aluminum (Al), titanium (Ti), iron (Fe), nickel (Ni), and gold (Au). Here we use Ti as the BCE because the work function of Ti and the electron affinity of TiO_2 is close to -4.1 and -4.2 eV, respectively, and thus the Ti/TiO_2 interface form an Ohmic contact which is essential for smooth electron transfer thorough the interface. Ti was also found to maintain good stability on TiO_2 film in electrolyte with I^-/I_3^-.

Because the BCE of the BCDSC is located on the side opposite to light irradiation, the direction of electron transport in the TiO_2 film is thought to be reversed relative to the DSC and to therefore be the same as the direction of I_3^- transportation in the electrolyte solution, whereas in the DSC the directions of electron and I_3^- transportation are opposite. The probability of recombination between the injected electrons and I_3^- may therefore be higher in the BCDSC than the DSC. As redox couple transportation, electron collection efficiency, and dye adsorption onto the TiO_2 film are strongly affected by the properties of the BCE due to its porous structure and location between the TiO_2 film and the Pt counter electrode, it needs to have not only high conductivity and firm bonding to the TiO_2 film for efficient electron collection but also sufficient porosity for efficient dye adsorption and redox couple transportation.

For the purpose of developing a high-quality porous BCE film, we studied different deposition methods such as sputtering and vacuum deposition under different experimental conditions. We found that vacuum deposition was more efficient than other methods. Parts a and b of Figure 2 show scanning electron microscopy (SEM) images of the TiO_2 film surface and the TiO_2 porous film coated with Ti deposited for 300 s, respectively. Here we use Ti deposition time instead of thickness because of the difficulty of measuring the thickness of the BCE deposited on the porous TiO_2 surface. It was found that the pore size of the BCE decreases with increase in Ti deposition time. As shown in Figure 2b, the surface of the TiO_2 particles is fully coated with a thin layer of Ti in which, while many pores are still observed, both pore density and pore size are reduced compared to the uncoated TiO_2 film. From the SEM image of the Ti-coated film, the pore size is estimated to be about 10 nm, smaller than in the uncoated TiO_2 film, where average pore size distribution of 20−25 nm was estimated by Brunauer−Emmett−Teller (BET) measurement. Given that the sizes of the dye molecule (N719) and I_3^-, as calculated by the molecular orbital method using CaChe Ver. 5.0 with ZIND parameters, are about 14 and 7 Å, respectively, the BCE pore size of 10 nm is large enough for dye molecules to penetrate for efficient dye adsorption onto the nanocrystalline TiO_2 film and also for smooth I^-/I_3^- redox couple transportation through the BCE for the purpose of efficient hole transportation.
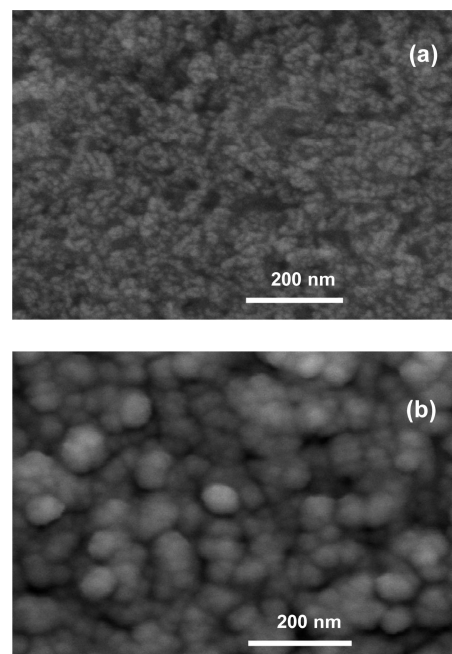

Figure 2. Scanning electron micrograph of surface of TiO_2 film. (a) TiO_2 porous film. (b) TiO_2 porous film coated with back contact electrode of titanium. Approximate pore radius of films: 25 nm (a), 10 nm (b). Scale bar: 200 nm.

In order to study the dye adsorption properties of the Ti-coated TiO_2 film, the amount of dye uptake was investigated on uncoated TiO_2 film and on Ti-coated TiO_2 films using Ti deposition times varying between 200 and 700 s. It was found that the amount of dye adsorbed onto Ti-coated TiO_2 film remained constant at Ti deposition times of up to 600 s and then decreased with further increase in deposition time. Dye adsorption values of 1.11×10^{-7} and 1.05×10^{-7} mol cm^{-2}, were estimated for TiO_2 film with Ti deposition time of 600 s and for uncoated TiO_2 film, respectively, under the same dye adsorption conditions. The amount of dye adsorption in the BCDSC was almost the same as in the DSC. This result shows that, at Ti deposition times of up to 600 s, dye adsorption is not affected by the BCE structure of the BCDSC and confirms similarly efficient dye adsorption onto the TiO_2 surface as in the DSC.

It is known that the conversion efficiency (η) of solar cells can be represented as follows:[18]

$$\eta = J_{SC}V_{OC}FF/P_{in} \tag{1}$$

where FF, J_{SC}, V_{OC}, and P_{in} are the fill factor, short-circuit current density, open-circuit voltage, and incident power, respectively.

In a previous paper, we investigated the internal resistance of DSCs through EIS measurement and observed four resistance elements. Of these four, the three resistance elements related, respectively, to the charge-transfer processes at the Pt counter electrode, the ionic diffusion in the electrolyte, and the sheet resistance of TCO and the contact resistance between the TCO and TiO_2 showed a series-internal resistance behavior which affects FF. The fourth resistance element, related to the charge transfer at the $TiO_2/$

(18) Sze, S. M. *Physics of Semiconductor Devices*, 2nd ed.; John Wiley & Sons: New York, 1981.
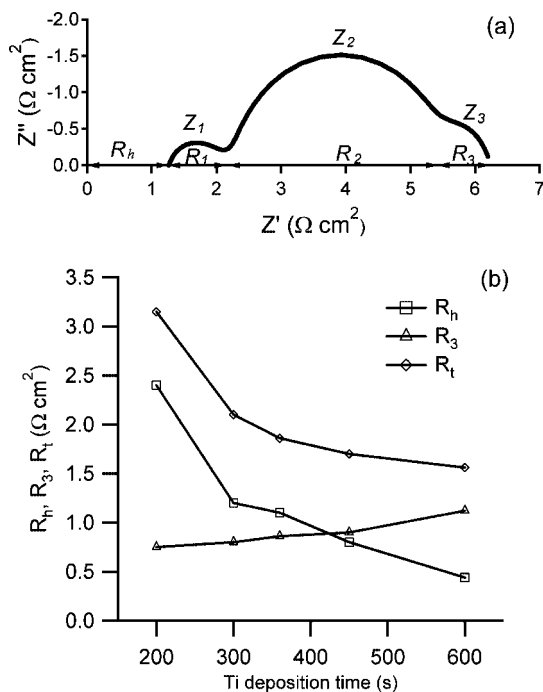
Figure 3. (a) Electrochemical impedance spectrum (EIS) of the back contact dye-sensitized solar cell with Ti deposition time of 300 s. (b) Dependence of Ti deposition time in back contact dye-sensitized solar cells on redox transport resistance (R_3), electron transport resistance (R_h), and total resistance (R_t) of R_h and R_3 estimated by EIS.

dye/electrolyte interface, was found to resemble the resistance of a diode, as it was dependent on the applied bias voltage.

As the redox couple diffusion in the electrolyte and the electron transportation through the porous Ti network are dependent on the properties of the BCE, an EIS technique was applied to study and optimize the role of the BCE in BCDSC operation.[19,20] The internal resistance of BCDSCs with Ti deposition time of between 200 and 600 s was investigated

Figure 3a shows the electrochemical impedance spectrum of a BCDSC with Ti deposition time of 300 s. Three semicircles were observed in the spectrum, and the response frequency of each semicircle was similar to those reported earlier for DSCs by our group.[19] These semicircles are attributed to the redox reaction at the platinum counter electrode (Z_1, frequency regions 10^3-10^5 Hz), the electron transfer at the TiO$_2$/dye/electrolyte interface (Z_2, frequency regions $1-10^3$ Hz), and the redox transport within the electrolyte (Z_3, frequency regions $10^{-1}-1$ Hz). The resistance elements R_1, R_2, and R_3 are described as the real part of Z_1, Z_2, and Z_3, respectively. The resistance element R_h in the high-frequency range over 1 MHz is influenced by the sheet resistance of BCE and the contact resistance between the BCE and TiO$_2$.[21,22] Both R_h and R_3 were observed to be strongly dependent on the Ti deposition time. It is necessary to minimize both R_h and R_3 to improve FF; on the other

(19) Han, L.; Koide, N.; Chiba, Y.; Mitate, T. *Appl. Phys. Lett.* **2004**, *84*, 2433.
(20) Kern, R.; Sastrawan, R.; Ferber, J.; Stangl, R.; Luther, J. *Electrochim. Acta* **2002**, *47*, 4213.
(21) Han, L.; Koide, N.; Chiba, Y.; Islam, A.; Komiya, R.; Fuke, N.; Fukui, A.; Yamanaka, R. *Appl. Phys. Lett.* **2005**, *86*, 213501.
(22) Han, L.; Koide, N.; Chiba, Y.; Islam, A.; Mitate, T. *C. R. Chim.* **2006**, *9*, 645.
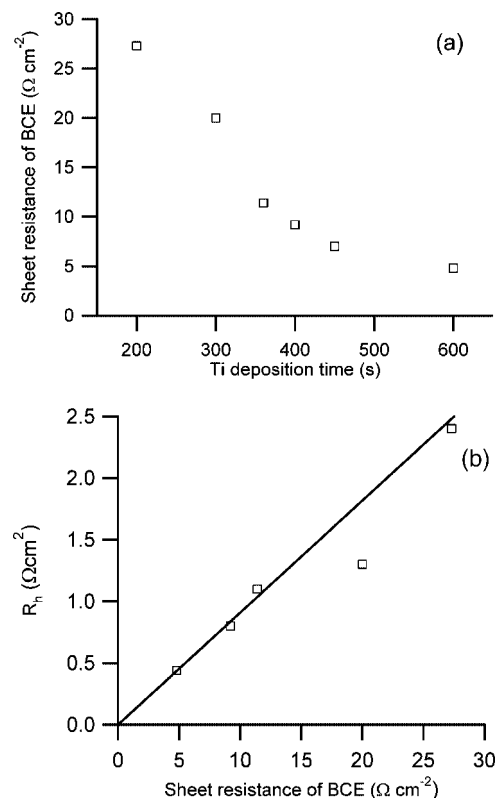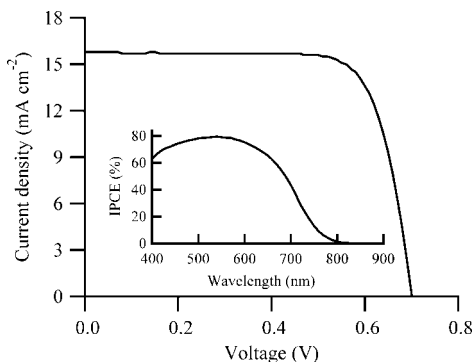
Figure 4. (a) Dependence of Ti deposition time on sheet resistance of the back contact electrode. (b) Relationship between sheet resistance and R_h. The solid line indicates the result of the line fit.

hand R_1 was found to be nearly constant throughout the experiment because the same Pt counter electrode was used and R_2 acts as a diode and does not affect series resistance.

Figure 3b shows the dependence of redox transport resistance (R_3) and BCE resistance (R_h) on Ti deposition time. It was found that I$^-$/I$_3^-$ redox transport resistance increased with increase in Ti deposition time because the BCE pore size decreased. BCE resistance (R_h), on the other hand, decreased with increase in Ti deposition time due to the increase in the thickness of the BCE. As FF is known to be inversely proportional to internal series resistance, it is important to optimize the thickness of BCE to obtain high FF. Figure 3b also shows the dependence on Ti deposition time of R_t, R_h, and R_3. It was found that Ti deposition time of around 600 s produces the minimum series resistance. As the amount of dye uptake decreased at Ti deposition times of over 600 s, the optimum Ti deposition time was considered to be 600 s in the present experiment.

Next, the sheet resistance of BCE was confirmed using the four-point probe method. Figure 4a shows the dependence of BCE sheet resistance on Ti deposition time. The BCE sheet resistance decreases with increasing Ti deposition time. This tendency is similar to the dependence of R_h on Ti deposition time as shown in Figure 3b. Figure 4b shows the dependence of R_h on BCE sheet resistance and indicates that R_h is proportional to BCE sheet resistance. This result also suggests that R_h is mainly due to BCE sheet resistance. The contact resistance between the BCE and the TiO$_2$ film is expected to be much smaller as the approximated line in Figure 4b passes through the (0, 0) point, suggesting that the BCE is firmly bonded to

Figure 5. Current−voltage characteristics of BCDSC with N719 dye. The result was measured at 25 °C with an aperture area of 0.2209 cm² using a metal mask, irradiance of 100 mW cm⁻², and scan mode from J_{SC} to V_{OC}. J_{SC} = 15.8 mA/cm², V_{OC} = 0.701 V, FF = 0.758, η = 8.4%. The incident photon-to-current efficiency (IPCE) of the BCDSC is also shown as an inset. A maximum IPCE of almost 80% was obtained.

the TiO₂ surface. The sheet resistance of BCE at a Ti deposition time of 600 s showed a very low value of 5 Ω cm⁻², which is even lower than the value of around 10 Ω cm⁻² found in the TCO substrate usually used in DSCs.

Figure 5 shows the current−voltage characteristics of a BCDSC with optimized BCE and N719 dye under AM 1.5 sunlight illumination. The values of J_{SC}, V_{OC}, and FF are 15.8 mA cm⁻², 0.701 V, and 0.758, respectively, yielding an overall energy conversion efficiency of 8.4%. The electrochemical impedance spectrum of the optimized BCDSC shows a redox couple transport resistance (R_3) of 1.1 Ω cm² and BCE resistance (R_h) of 0.45 Ω cm². The corresponding values of R_3 and R_h observed in conventional DSCs are approximately 0.5 and 1.1 Ω cm², respectively. The value of R_h observed for the BCDSC is lower than that for the DSC because of the successful fabrication of a BCE with low sheet resistance of 5 Ω cm⁻² as against the TCO sheet resistance of 10 Ω cm⁻². However, the R_3 value of the BCDSC was higher than that of the DSC because of the former's smaller pore size, which suppressed redox couple movement. These results are well-consistent with the experimental results displayed in Figures 3 and 4. A maximum IPCE of 80% at around 550 nm is obtained in the BCDSC and is similar to that in the DSC. The transmittance of the light irradiated substrate in the BCDSC is over 90% because of the omission of the TCO, which decreases transmittance by about 10% due to light absorption. It should thus be possible to improve IPCE to more than 90% in the BCDSC. We succeeded thus in fabricating a BCE with lower sheet resistance than TCO. In this way, through improvement of J_{SC} and FF, the BCDSC offers higher potential than the DSC for the construction of an efficient cell.

In polycrystalline silicon, there are many deep traps located at the grain boundary between the crystals where carriers are trapped and loss occurs via the recombination process. The carrier lifetime in polycrystalline silicon is much shorter than in monocrystalline silicon. For a BCS structure, lifetime must be long enough for the carrier to travel through the cell as far as the back contact. The BC structure cannot therefore be used in a solar cell of
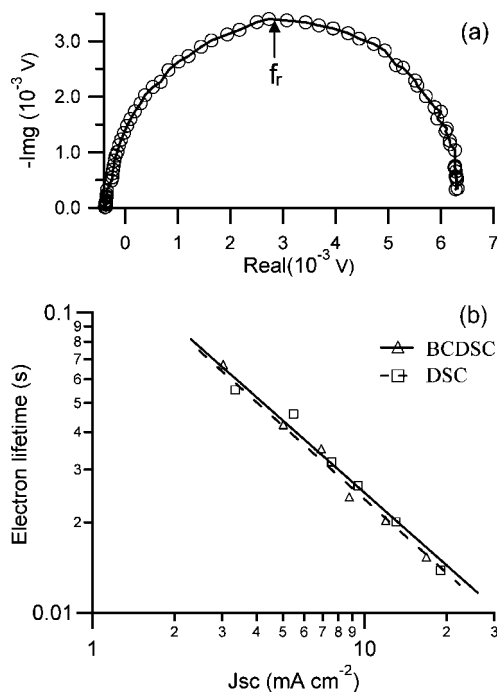

Figure 6. (a) Typical intensity modulated photovoltage spectroscopy (IMVS) response in the complex plane for BCDSC. (b) Comparison of electron lifetime estimated by IMVS for the BCDSC and DSC at short-circuit current density (J_{SC}) under simulated solar light.

polycrystalline silicon. In monocrystalline solar cells of BC structure, meanwhile, conversion efficiency depends strongly on carrier lifetime.[23]

As shown in Figure 5, however, the BCDSC in the present study showed a high shunt resistance of 2000 Ω cm² which was estimated from the I−V curve, V_{OC} of the same value as in the DSC at 0.7 V, and high conversion efficiency. The high value of shunt resistance and V_{OC} of BCDSC indicates a slow electron-transfer rate from TiO₂ to electrolytes. In order to investigate the reason why the BCDSC showed high conversion efficiency and slow electron-transfer rate despite the use of polycrystalline TiO₂, we measured the electron lifetime of the BCDSC and DSC with the same thickness of TiO₂ film using IMVS.[15,16] Figure 6a shows a typical IMVS response curve for the BCDSC. The IMVS plots display a semicircle in the complex plane similar to that observed with DSCs.[15] This result suggests that the IMVS analytical method used for DSCs could be applied to BCDSCs. The electron lifetime (τ) can be estimated using the following equation:

$$\tau = 1/2\pi f_r \qquad (2)$$

where f_r is the characteristic frequency minimum of the imaginary component of the IMVS response in the complex plane. For a specific value of electron density in TiO₂ (J_{SC}), the electron lifetime (τ) is calculated using eq 2, where f_r is measured from the IMVS plot as shown in Figure 6a. Figure 6b shows the dependence of electron lifetime on J_{SC}. The electron lifetime of both DSC and BCDSC decreased with increase in J_{SC} as the number of electrons in the conduction band of TiO₂ increases and more electrons therefore reach the recombination site on

(23) McIntosh, K. R.; Cudzinovic, M. J.; Smith, D. D.; Mulligan, W. P.; Swanson, R. M. *Proceedings of the 3rd World Conference on Photovoltaic Energy Conversion*, Osaka, Japan, May 2003; p 971.

the surface of the TiO_2 particle. As shown in Figure 6b, it was found that the electron lifetime in BCDSC was similar to that in DSC at all values of J_{SC}. This result suggests that, although the electron and the hole (I_3^-) move in the same direction, electron lifetime is not affected by grain boundaries or losses via the recombination process. The results can also be explained by the different structures of the DSC and silicon solar cell: in the former, the injected electron and the hole transporter (I_3^-) are transported in separate materials, the electron in the TiO_2 particle network and I_3^- in the electrolyte solution, whereas in the latter electron and hole are transported in the same material. It is therefore likely that electron lifetime in the BCDSC is not very different from that in the DSC. In polycrystalline silicon, on the other hand, electron and hole are present in the same material and lifetime decreases significantly due to the recombination process when the carrier moves across the grain boundary.

Conclusions

We succeeded in constructing a low-cost BCDSC in which a porous metal layer is used as a BCE instead of the TCO electrode used in the conventional DSC. It was confirmed that the BCE needs to have not only enough pores for efficient I^-/I_3^- redox couple transportation through the pores but also low sheet resistance for efficient electron collection. Optimization of the BCE is therefore a key factor for improving the efficiency of the BCDSC. Finally, an optimized BCDSC was fabricated which displayed conversion efficiency of 8.4%. The investigation of electron lifetime indicated that the electron lifetime in nanocrystalline TiO_2 film was almost the same in the BCDSC as in the DSC, which is long enough for efficient electron collection. This low-cost and efficient BCDSC without a TCO has strong potential for practical application.